Collapse of the Atlantic Meridional Overturning Circulation (AMOC)

Louis Forrester

April 2024

Abstract

This paper presents methods for solving a stochastic differential equation (SDE) which describes the Atlantic meridional overturning circulation (AMOC). Both numerical and analytical techniques for solving the SDE are considered, and their effectiveness for describing the probability density of states which the AMOC can exist in, are evaluated. A toy model, [1] is used to demonstrate the switching of the AMOC states. Variables, σ and T that govern these states are explored, and limits on values of these variables are discussed. The environmental impact of these tests are used in conjunction with alternative models to discuss what can be done to prevent the AMOC from collapsing.

1 Introduction

The Atlantic Meridional Overturning Circulation (AMOC) is an ocean current system that transports warm equatorial waters into the North Atlantic, and plays a crucial role in regulating the Earth's climate and distributing heat across the globe.
The AMOC is driven by differences in temperature and salinity, which affect the density of seawater. As warm water flows northward, it cools and salinity increases due to evaporation, increasing its density. This dense water then plunges deep into the ocean depths and slowly spreads southward, several kilometers below the surface. Eventually, this cold, dense water is drawn back up to the surface through a process called "upwelling," where it warms and completes the circulation cycle. This continuous mixing of the world's oceans ensures that heat and energy are distributed evenly across the planet, contributing to the climate experienced on Earth.
Continuous monitoring of the AMOC since 2004 has revealed year-to-year variations that likely influence weather patterns in the UK. Prior to 2004, Oceanographers relied on indirect evidence, such as sediments on the seafloor, to measure the AMOC. While the indirect evidence is not always consistent, it is understood that the AMOC has undergone significant and rapid changes in the past, particularly around the end of the last ice age.
Climate models predict that the AMOC will weaken over the 21st century as greenhouse gas concentrations increase. As the atmosphere warms, the surface ocean retains more heat, and increased rainfall and ice melt make it fresher. These changes make the ocean water lighter, reducing the effects of upwelling, and weakening the AMOC. This weakening of the AMOC could have far-reaching consequences for the global climate, potentially leading to cooler temperatures in Europe and disruptions to weather patterns worldwide. Monitoring and understanding the AMOC is crucial for predicting and mitigating the impacts of climate change on this vital ocean current system.

2 The collapse of the AMOC

The Atlantic Meridional Overturning Circulation (AMOC) exhibits abrupt transitions between its active "on" state and a weakened "off" state. The influx of substantial meltwater from Greenland and the Arctic regions is considered the primary driver behind the shift from the "on" to the "off" state of the AMOC. Alarmingly, recent observations indicate that the AMOC has undergone a significant slowdown.

2.1 Modeling the AMOC's Tipping Point

To explore the factors that affect the AMOC's switching behavior, a simplified "toy model" has been introduced, based on a type of stochastic differential equation called an Itô equation. This model is outlined below,

$$dX_t = -\frac{dU}{dX}(X_t; T)\, dt + \sigma dW_t. \tag{2.1.1}$$

Here, X, a random variable, represents the strength of the AMOC. T is the freshwater forcing (i.e., the influx of meltwater), and σ is the noise amplitude, representing the inherent variability of the system. U is the potential defined by [1],

$$U(X_t; T) = \frac{X^4}{4} - \frac{X^2}{2} + TX. \tag{2.1.2}$$

2.2 Tipping Points

This model exhibits two stable states: a strong AMOC (positive X) and a weak AMOC (negative X). As the freshwater forcing T increases, the system approaches a tipping point, beyond which the strong AMOC state becomes unstable, and the system transitions to the weak state. The noise term σdW introduces random fluctuations, which can occasionally push the system past the tipping point, even before the critical freshwater forcing is reached. This phenomenon, known as noise-induced tipping, highlights the potential for abrupt and unexpected transitions in the AMOC's behavior. By studying this toy model, insights into the factors that govern the AMOC's stability and the conditions under which it may undergo a catastrophic collapse can be gained.

2.3 Potential Landscape and Steady States

For specific values of T, the potential energy landscape of the system behaves differently. When $T = 0$, the potential assumes the form displayed in Figure 1. The system is effectively in a steady state, where switching occurs between the "on" state and the "off" state. This demonstrates that the physical parameter T controls the switching behavior. If T becomes greater than zero, the system falls into a positive state, as outlined in Figure 3. Conversely, if T becomes less than zero, the system transitions to a negative state, as shown in Figure 2.

These potential energy landscapes provide valuable insights into the behavior of the AMOC system and the role of the freshwater forcing parameter T in determining its stability and potential for abrupt transitions. By solving this Itô equation, one can extract the probability of finding the solution in a particular state. Numerical and analytical approaches will be considered to obtain this probability.

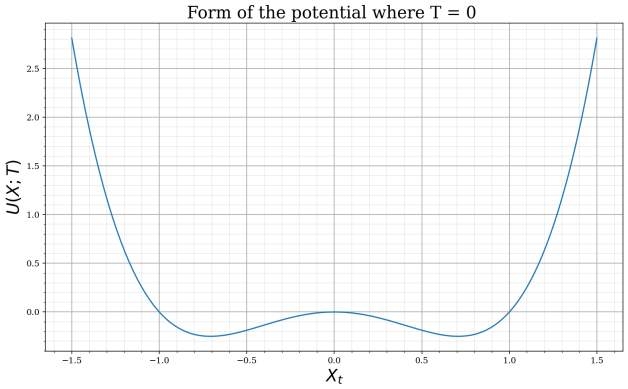

Figure 1: The potential when $T = 0$.

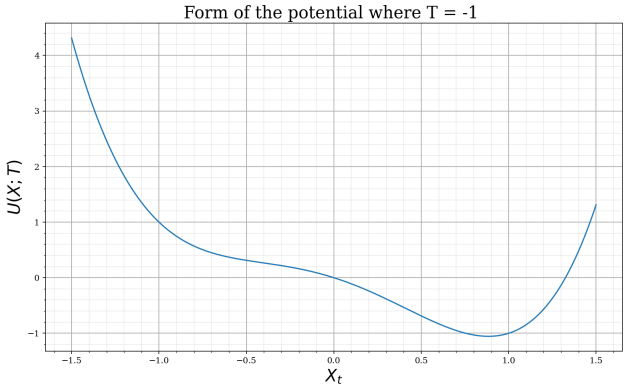

Figure 2: The potential when $T < 0$.

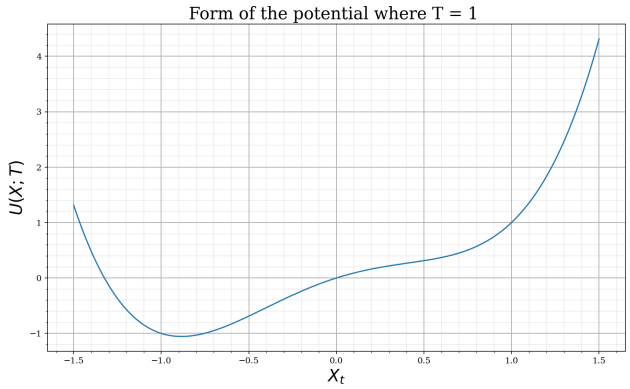

Figure 3: The potential when $T > 0$.

3 Numerical Method: Monte-Carlo Simulation

A Monte-Carlo simulation can be used to determine the probability density of the Itô equation. A Monte-Carlo simulation runs thousands of different events, in this case, it simulates finding the solution to the Itô equation, and sorts the results according to how many times they occur in a histogram plot, for a specified time interval, and N events. In all cases of T below, the time interval is set to $t_f = 10s$, and the number of events, N = 100,000. The larger the number of events, the smaller the error of the simulation. The error follows the relationship,

$$\epsilon \propto \frac{1}{\sqrt{N}}. \tag{3.0.1}$$

For $N = 100,000$, $\epsilon \propto 3.16 \times 10^{-3}$. The N and t parameters are related according to,

$$t = Ndt \rightarrow dt = \frac{t}{N} = \frac{10}{50000} = 0.0001. \tag{3.0.2}$$

This dt then defines the variance of the normal distribution described by dW. This choice of event number and time scale lead to a normal distribution with variance $\sqrt{dt} = 0.014$, and a mean of zero.

Here, T values which describe states as on, off or switching. For $T = -1$. The $X(t)$ values are positive, so will take this state to be the on-state. This therefore makes negative $X(t)$ values the off-state, where $T = -1$. The remaining *state* will be regarded as a pseudo-state as it is technically not a state, it is a linear combination of two states which have an equal probability. This is the switching state, or the unstable state. By fitting a curve to the histogram, probability density can be found. However, multiple fitting techniques can be applied to find this. Here, two fittings were considered, least mean square (LMS), and orthogonal distance regression (ODR).

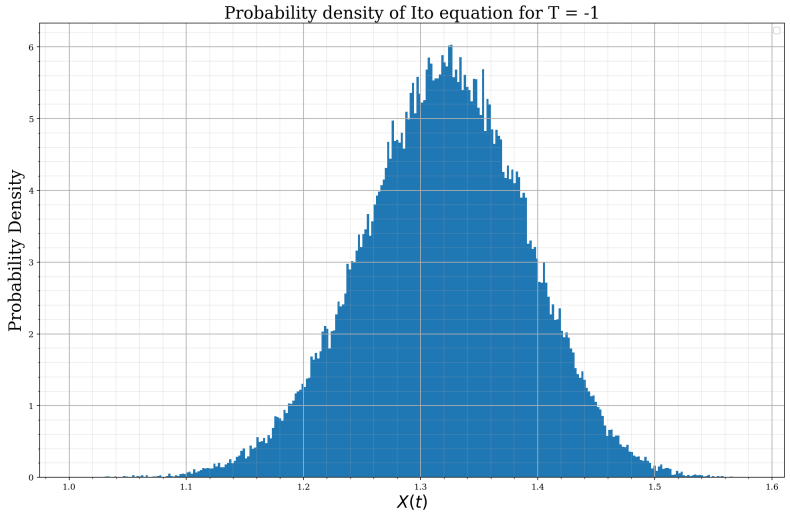

Figure 4: Probability density of position when $T = -1$, $\sigma = 0.2$. Here there is one distinct peak, corresponding to the on state.

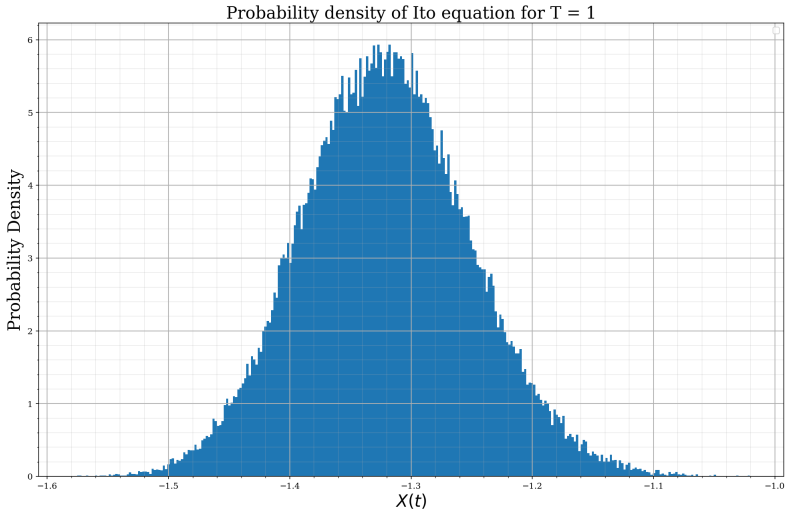

Figure 5: Probability density of X_t when $T = 1$, $\sigma = 0.2$. Here there is one distinct peak, corresponding to the off state.

LMS finds the best-fit curve or line that minimizes the sum of the squared differences between the observed data points and the fitted values from a model. Here the model was gaussian in form, and starting parameters were guesses from observation. The LMS then determines the best parameters by iterating over many times, until a stop condition was met, or the residuals between the model and the distribution were sufficiently small. ODR is a similar process but it accounts for errors in both predictor and response variables by minimizing the orthogonal distances, while LMS assumes errors only in the response variable and minimizes the vertical distances.

Figure 7 demonstrates the difference between the two fitting methods. The curve-fit, using LMS, is clearly a better fit as it wraps around the distribution more tightly compared to the ODR method which seems to overestimate the height of the function and offsets the mean slightly too far to the left. This is likely due to the fact that ODR is taking the random fluctuations as errors, whilst LMS ignores this. Computing the curve several times also produced different results for the ODR method, whilst the LMS method consistently calculated similar ideal parameters. Finally, to verify that this distribution was correctly normalised, the area under the curve was calculated using scipy quad. For each state, the distribution summed to

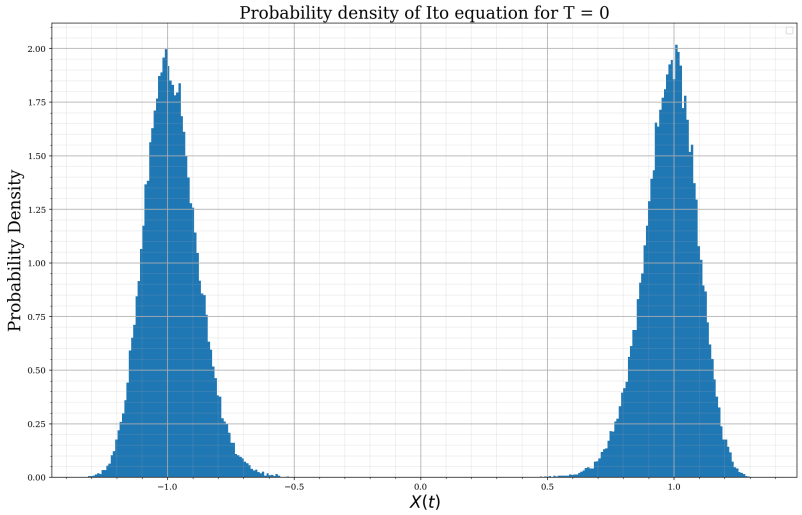

Figure 6: Probability density of X_t when $T = 0$ (unstable state), $\sigma = 0.2$. Here there are two distinct peaks of similar area.

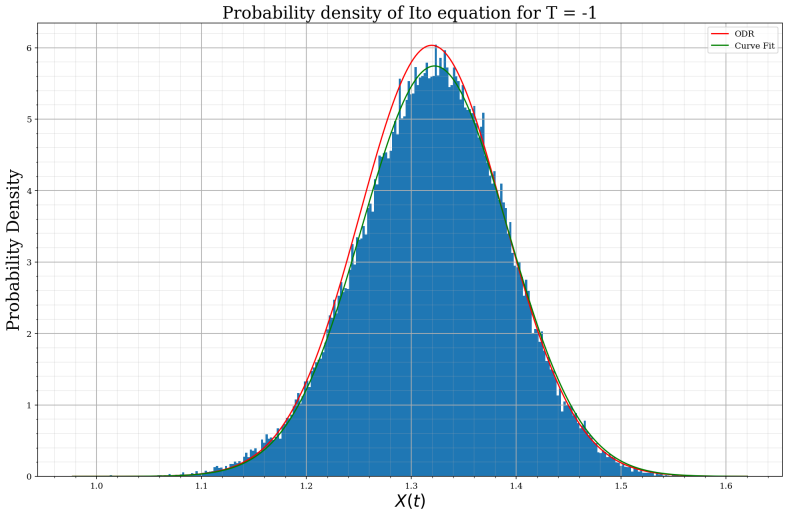

Figure 7: The distribution function for $T = -1$ (on-state), $\sigma = 0.2$, with both ODR and LMS fitting applied.

$0.9999 \approx 1$, indicating that this accurately described the probability density of $X(t)$.

3.1 Understanding the effects of varying σ

The figures stated above, all use the same parameters for N, t and σ. σ, which is the height of the normal distribution, dW, was arbitrarily chosen to be 0.2. The physical interpretation of this value could be a range of different factors such as pressure, ambient temperature, wind or current speed. In this investigation, σ represents the magnitude of the random fluctuations of $dX(t)$.

3.1.1 Steady state for varying σ

Here several values of σ are shown to demonstrate how increasing σ increases the spread of the gaussian which describes the state. For $\sigma = 0$, the random fluctuations in X_t are zero, resulting in a purely deterministic simulation. This produces a Dirac-delta function centered around the mean and effectivley describes a situation where X_t does not change, and is constant in time.

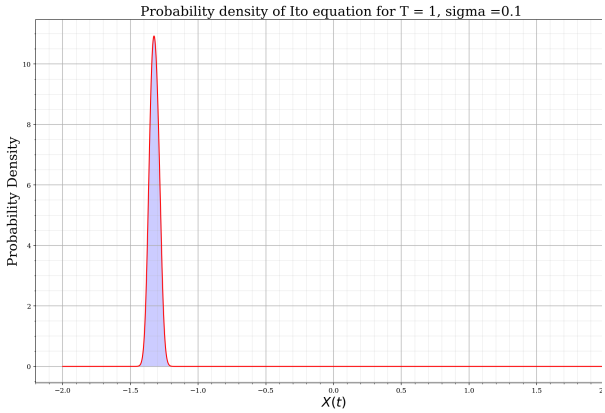

Figure 8: Probability density for off state. $T = 1$, $\sigma = 0.1$

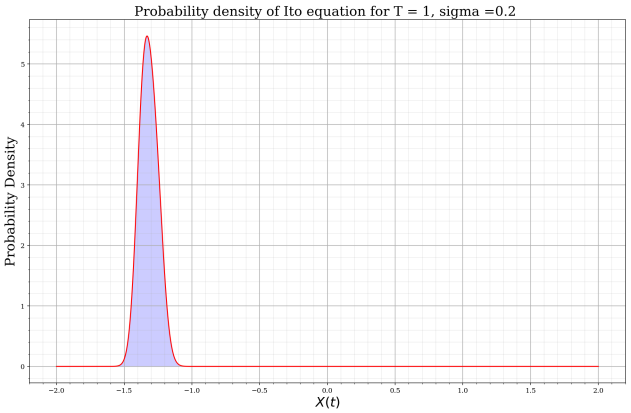

Figure 9: Probability density for off state. $T = 1$, $\sigma = 0.2$

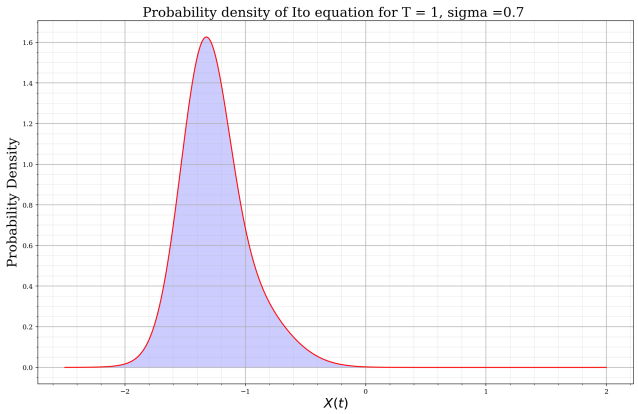

Figure 10: Probability density for off state. $T = 1$, $\sigma = 0.7$

Increasing σ to 0.1, as shown in figure 8 and using the Monte-Carlo simulation to calculate the probability of finding $X(t)$ in the off state yields,

$$P(-1.5 \leq X(t) \leq 0) = 0.999, \text{ and the on-state, } P(0 \leq X(t) \leq 1.5) = 0.0 \tag{3.1.1}$$

This concludes that with these conditions, the AMOC is off with no probability of switching to the on state. However, by increasing σ slightly to 0.2, the gaussian describing the state spreads out shown in 9. In figure 9, the gaussian is slightly broader. Re-calculating the probability of finding X_t in the same ranges as the previous σ,

$$P(-1.5 \leq X(t) \leq 0) = 0.998, \text{and}, P(0 \leq X(t) \leq 1.5) = 5.751e-108 \pm 1.12e-107 \tag{3.1.2}$$

shows that, values of σ beyond $\sigma = 0.1$ tip the probability of finding X_t in the off state to non-zero. Obviously, this probability is incredibly low, so can be taken to be zero, but this shows how sensitive the calculations are in stochastic processes. For a more extreme case, where $\sigma = 0.7$ in figure 10, the probability is,

$$P(-1.5 \leq X(t) \leq 0) = 0.99974, P(0 \leq X(t) \leq 1.5) = 0.00025. \tag{3.1.3}$$

This σ is more reasonable in this physical system as whilst the probability of switching is low, it is no longer statistically impossible.

Therefore, by increasing the magnitude of the random fluctuations of the stochastic equation, one can increase the probability that said random fluctuation can push the AMOC to switch states. This becomes more pressing when $T \to 0$, and the two peaks are produced.

3.1.2 Unstable state for varying σ

$T = 0$ represents a scenario where the AMOC has an equal probability of being in the off-state as it does the on state. In this state, the distribution has a region where the states overlap. This is dangerous as there is a higher probability of switching from one state to another. In reality, there must be two distinct states when $T = 0$, therefore, $\sigma = 0.7$ is too high. Finding the the ideal value for σ is achieved by looping over different values until $P(-0.2 \leq X(t) \leq 0.2) = 0$, as this is the maximum value for which the two states are deemed to be distinct. This occurs at $\sigma = 0.35$ as shown in figure 12.

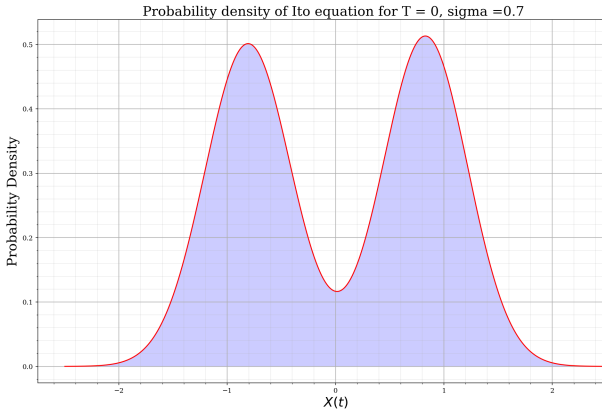

Figure 11: Probability density for unstable state. $T = 0$, $\sigma = 0.7$

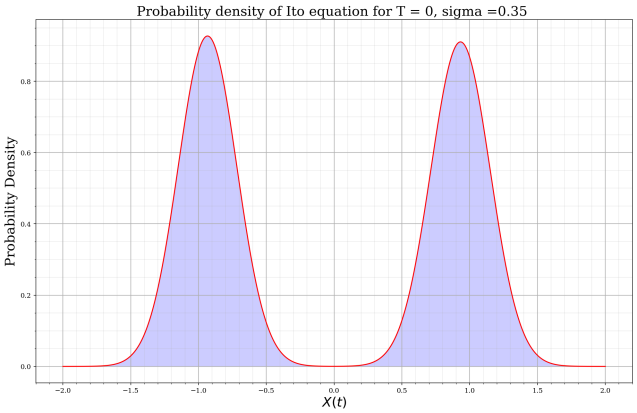

Figure 12: Probability density for off state. $T = 1$, $\sigma = 0.35$

Now that a 'good' value for sigma has been agreed upon, it is sensible to expose the system to changes in the control parameter, T.

3.2 Understanding the effects of varying T

T physically represents an analogue for the global temperature of Earth. In reality it is a far more complicated than a temperature scale but for the sake of simplicity, it will be referred to as a variable which is controlled by the temperature. Negative T values correspond to temperatures cooler than present-day conditions, promoting the 'on' state of the AMOC. $T = 0$ represents the current baseline temperature, while positive T values indicate warmer temperatures that can destabilize the AMOC and push it towards the 'off' state .

3.2.1 Stable states for varying T

Cases where $T = \pm 0.1$ are shown in figure 14 and figure 13.

In figure 13 and figure 14, the probabilities of each state are symmetric. Here, for positive T,

$$P(-2.5 \leq X(t) \leq 0) = 0.6937, P(0 \leq X(t) \leq 2.5) = 0.3063, \tag{3.2.1}$$

whereas for negative T,

$$P(-2.5 \leq X(t) \leq 0) = 0.3076, P(0 \leq X(t) \leq 2.5) = 0.6924. \tag{3.2.2}$$

This proves that this model is symmetric for T.

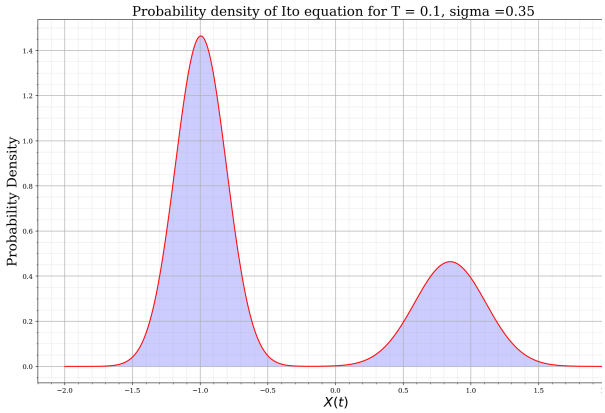

Figure 13: Probability density for intermediate state. $T = 0.1$, $\sigma = 0.35$

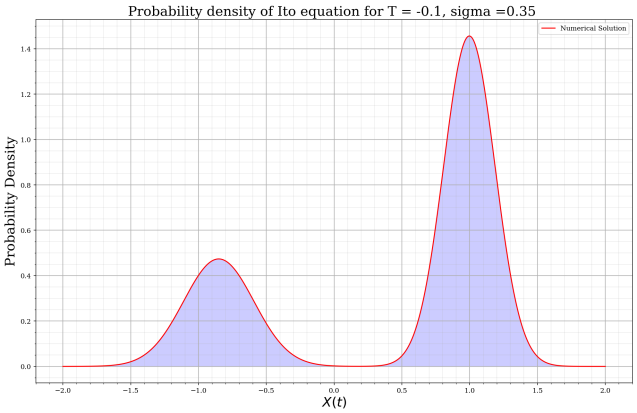

Figure 14: Probability density for intermediate state. $T = -0.1$, $\sigma = 0.35$

3.2.2 Critical state

To observe the steady state, T must be fixed to zero a discussed. However, the fitting for the distribution in the steady state is not quite as good as previously expected. Therefore, alternative methods must be sought to accurately find the probability in the steady state.

3.3 Finding the tipping point

Finding the probability of each state for a range of T between $-1 \leq T \leq 0$ and arranging them in a table means that the critical values for T can be found which cause the probability for tipping to increase.

T	$P(+$ AMOC$)$	P(-AMOC)
-1	0.999	≈ 0
-0.5	0.999	$1.5E-08$
-0.45	0.996	0.004
-0.4	0.990	0.01
-0.3	0.950	0.05
-0.2	0.852	0.148
-0.1	0.691	0.309
0	0.501	0.499

Table 1: Small changes in T which become more positive show reductions in the probability of the AMOC existing in a positive state, whilst the probability for negative AMOC increases. Due to the symmetry of the system, the P(+AMOC) values for $T \geq 0$ will match the P(-AMOC) for $T \leq 0$. Plots for these values can be found in appendix A.

Table 1 displays the probability for both positive and negative states of the AMOC for a given values of T. It demonstrates that as the value of $T \to 0$, the probabilities tend to even out. It also shows that the sensitive region is $-0.5 \leq T \leq -0.4$. This means that for any values of T close to this range, there is a small probability for switching to occur. Obviously more negative values which tend to 1 are safest and the probabilities are closer enough to 1 for the positive AMOC. A graphical representation of the data is summarised in, figure 15.

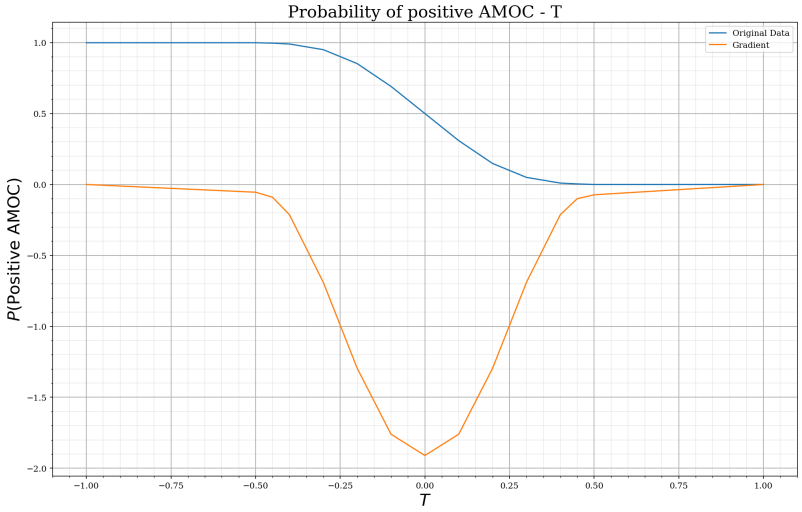

Figure 15: Probability of positive AMOC as a function of T. The orange curve represents the gradient of this curve.

Figure 15 demonstrates how the switching of the states occur when T is varied from -1 to 1. Here the critical region defined by the point where the gradient different from zero. This is clear to be where $T = -0.45$. (N.B - Inverting this gradient would appear to recover the probability density which perhaps is the consequence of the continuity equation) which reinforces the prediction made earlier. Due to the symmetry of the probabilities, the negative AMOC probability will be of the same form but in reverse. To make sense of these solutions, alternative approaches to calculating ρ must be explored.

4 Analytical Method

4.1 Fokker-Planck equation

An alternative analytical method can be used to determine the probability density. This can be achieved by finding the corresponding Fokker-Planck equation of the Itô equation, which has the effect of turning the *Itô* equation into a diffusion equation. A generic Itô equation,

$$dX_t = -\mathcal{A}\left(X_t; T\right)\rho dt + \mathcal{B}\left(X_t; T\right)\rho dW_t, \tag{4.1.1}$$

has a corresponding Fokker-Planck equation of the form,

$$\frac{\partial \rho}{\partial t} = -\frac{\partial}{\partial x}\left(\mathcal{A}\left(x,t\right)\rho\right) + \frac{1}{2}\frac{\partial^2}{\partial x^2}\left(\mathcal{B}\left(x,t\right)\rho\right), \tag{4.1.2}$$

where ρ is the probability density. Rewriting this equation as a continuity equation by introducing the probability flux, $\mathcal{F}$,

$$\frac{\partial \rho}{\partial t} + \frac{\partial \mathcal{F}}{\partial x} = 0, \tag{4.1.3}$$

where $\mathcal{F}$ is defined as,

$$\mathcal{F} = -\frac{1}{2}\frac{\partial}{\partial x}\left(\mathcal{B}^2\left(x,t\right)\rho\right) + \mathcal{A}\left(x,t\right)\rho. \tag{4.1.4}$$

The toy model has an associated continuity condition given by,

$$\frac{\partial \mathcal{F}}{\partial X_t} + \frac{\partial \rho}{\partial t} = 0, \tag{4.1.5}$$

where,

$$\mathcal{F} = -\frac{\sigma^2}{2}\frac{\partial}{\partial X_t}\rho\left(X_t;t\right) - \frac{dU\left(X_t;T\right)}{dX_t}\rho\left(X_t;t\right), \tag{4.1.6}$$

This leads to the following differential equation,

$$\frac{\partial \rho\left(X_t;t\right)}{\partial t} = \frac{d}{dX_t}U\left(X_t;T\right) + \frac{\sigma^2}{2}\frac{\partial^2}{\partial X_t^2}\rho\left(X_t;t\right). \tag{4.1.7}$$

Taking equation 4.1.6, and multiplying both sides by,

$$\exp\left(\frac{2}{\sigma^2}U\right), \tag{4.1.8}$$

yields,

$$\exp\left(\frac{2}{\sigma^2}U\right)\mathcal{F} = -\exp\left(\frac{2}{\sigma^2}U\right)\frac{\sigma^2}{2}\frac{\partial}{\partial X_t}\rho\left(X_t;t\right) - \exp\left(\frac{2}{\sigma^2}U\right)\frac{dU\left(X_t;T\right)}{dX_t}\rho\left(X_t;t\right). \tag{4.1.9}$$

Which can be simplified using the inverse product rule to make,

$$\exp\left(\frac{2}{\sigma^2}U\right)\mathcal{F} = -\frac{2}{\sigma^2}\frac{\partial}{\partial X_t}\left[\exp\left(\frac{2}{\sigma^2}U\right)\rho\left(X_t;t\right)\right], \tag{4.1.10}$$

rearranging,

$$-\frac{\sigma^2}{2}\exp\left(\frac{2}{\sigma^2}U\right)\mathcal{F} = \frac{\partial}{\partial X_t}\left[\exp\left(\frac{2}{\sigma^2}U\right)\rho\left(X_t;t\right)\right]. \tag{4.1.11}$$

4.2 The Steady State Solution

In the steady state, the probability flux $\mathcal{F}$ tends to zero as there is a zero probability that one state evolves in time to another. This therefore makes,

$$0 = \frac{\partial}{\partial X_t}\left[\exp\left(\frac{2}{\sigma^2}U\right)\rho\left(X_t;t\right)\right], \tag{4.2.1}$$

and hereby integrating with respect to X_t yields,

$$C = \exp\left(\frac{2U}{\sigma^2}\right)\rho \rightarrow C\exp\left(-\frac{2U}{\sigma^2}\right) = \rho, \tag{4.2.2}$$

which closely follows the steady state probability density derived using the numerical technique. By finding appropriate values for C, a good solution for the steady state can be determined. Comparing both the numerical and analytical solutions to to the histogram in figure 16, it appears as if the analytical solution is better suited for the steady state.

Figure 16 may also suggest that $\sigma = 0.35$ is not an ideal value for sigma as there is a small probability density present around $X_t = 0$. This indicates that the distribution has a non-zero flux, $\mathcal{F}$. In cases where this is true, the probability around $X_t = 0$ should be zero, as there should be two distinct states with no probability of switching. This revelation hints at a relationship between $\mathcal{F}$ and σ. But further research into this is required.

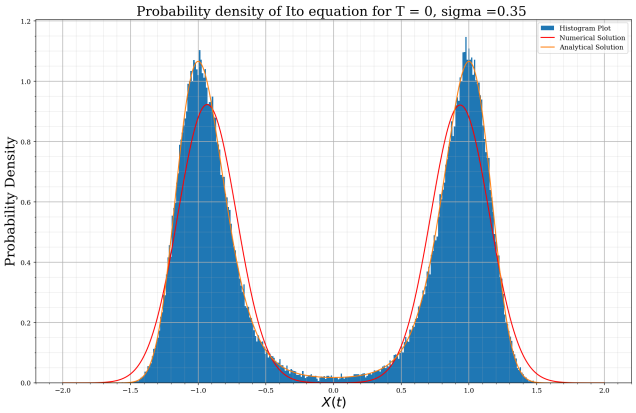

Figure 16: A comparison between the analytical and numerical fits to the steady state. The orange line is the analytical fit, the red line is the numerical fit, and the blue is the histogram.

5 Environmental consequences and ongoing research

With greenhouse gas emission on the rise, the global temperature is showing very clear signs of increasing. If the rate of global heating does not stop, then there is strong evidence that the AMOC will collapse. Due to the limitations of the model used, it is too difficult to accurately determine a window of time for which the collapse will occur, all that can be said for now is that if the control parameter T is a sufficient analogue for temperature, then an increase in this value leads to a negative AMOC state. Current assessments by the Intergovernmental Panel on Climate Change (IPCC) suggest that a full collapse is unlikely within the 21st century, [2]. However, they estimate a collapse of the AMOC to occur around mid-century under the current scenario of future emissions. Physics-based early warning signals [3] indicate that the present-day AMOC is onroute to tipping. Their early warning signal is a useful alternative to classical statistical ones, which according to their research, when applied to a simulated tipping event, turn out to be sensitive to the analyzed time interval before tipping. This indicates that an overall increase in T will prove catastrophic for the AMOC, it is unclear exactly what precautions, beside preventing a global warming, can be done to stop the AMOC collapsing.

6 Conclusion

The aims of this paper were to solve a stochastic differential equation which describes the deterministic and random properties of a variable X_t which describes the state of the AMOC. Using a toy model to describe the potential of the states that exhibits two minima (that is, stable equilibria or fixed points), it was determined that by changing the control parameter, T, representing an analogue for temperature, that the potential would collapse into one of two states. These states were referred to as On-states or Off-states, and represent the state of the AMOC. It was then found that changing T to either $+1$ or -1 would switch the AMOC off or on respectively. Once the nature of the switching was determined, the probability density of X_t could be found. To determine the probability density of X_t two methods, analytical and numerical were explored. Monte-Carlo simulations were used to determine the end value of X_t over a $100,000$ simulations after the system was allowed to evolve for $t = 10s$. This produced a histogram of the results which would differ according to the value of T. For $T = 0$, be two distinct peaks of equal height and width formed, indicating that when this condition is met, the probability of X_t existing in the off state and the on state is equally likely. For $T = \pm 1$, X_t would exist in either the on-state ($T = -1$) or the off-state ($T = 1$). To verify if the histogram correctly described the probability density, a model was fit to the curve. Two

fitting techniques were attempted, LMS and ODR. A comparison between the two showed that LMS was best as it fitted the histogram more closely, ignoring the larger fluctuations from the random component of the SDE. Calculating the area under the curve with limits $\pm\infty$ returned unity, proving that the distributions are correctly normalised. To ensure that the two states are distinct when $T = 0$, an upper limit on σ was found to be $\sigma = 0.35$. By slowly varying T from $-1 \leq T \leq 0$ in small intervals, a graph showing the probability as a function of T was found. The point where the probability of moving into the off-state became sufficiently large enough to cause concern for the AMOC was found to be between $-0.5 \leq T \leq -0.45$. Issues with the fitting occur when T was exactly zero and seemed to underestimate both the height and the width of the peaks. However, the analytical solution was able to correct these errors and prove very accurate when modelling the steady state. Future research into using the analytical solution for the On and Off states could be investigated to verify if the sensitivity range for T is accurate. If this sensitivity is in fact reached through the increased global temperature, the AMOC will eventually collapse into the off-state, which could have severe consequences to temperatures in western Europe.

References

[1] Niklas Boers. "Observation-based early-warning signals for a collapse of the Atlantic Meridional Overturning Circulation". In: *Nature Climate Change* 11.8 (Aug. 2021), pp. 680–688. DOI: 10.1038/s41558-021-01097-. URL: https://ideas.repec.org/a/nat/natcli/v11y2021i8d10.1038_s41558-021-01097-4.html.

[2] Peter Ditlevsen and Susanne Ditlevsen. "Warning of a forthcoming collapse of the Atlantic meridional overturning circulation". In: *Nature Communications* 14 (July 2023). DOI: 10.1038/s41467-023-39810-w.

[3] René M. van Westen, Michael Kliphuis, and Henk A. Dijkstra. "Physics-based early warning signal shows that AMOC is on tipping course". In: *Science Advances* 10.6 (2024), eadk1189. DOI: 10.1126/sciadv.adk1189. eprint: https://www.science.org/doi/pdf/10.1126/sciadv.adk1189. URL: https://www.science.org/doi/abs/10.1126/sciadv.adk1189.

A Plots

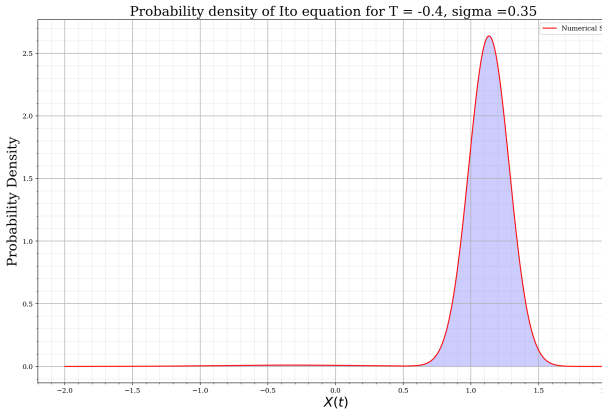

Figure 17: Probability density for intermediate state. $T = -0.4$, $\sigma = 0.35$

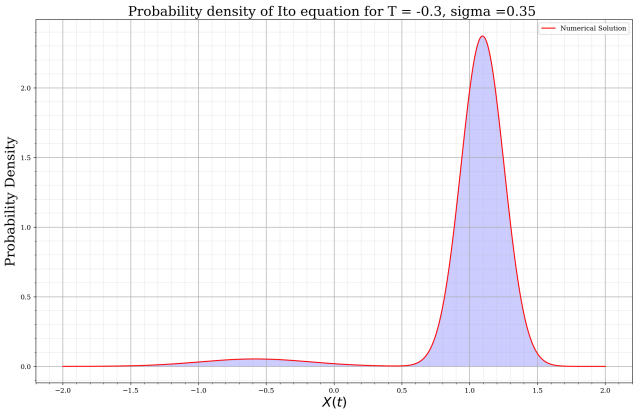

Figure 18: Probability density for intermediate state. $T = -0.3$, $\sigma = 0.35$

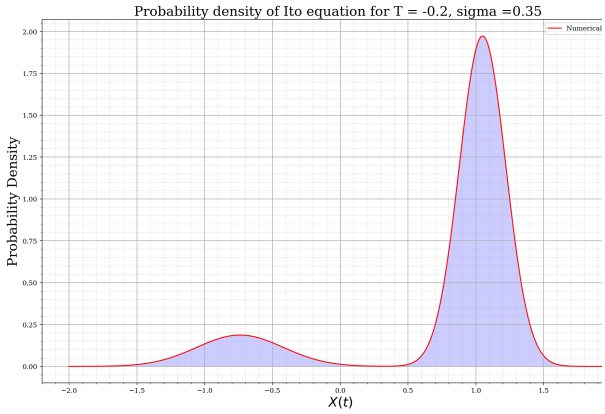

Figure 19: Probability density for intermediate state. $T = -0.2$, $\sigma = 0.35$

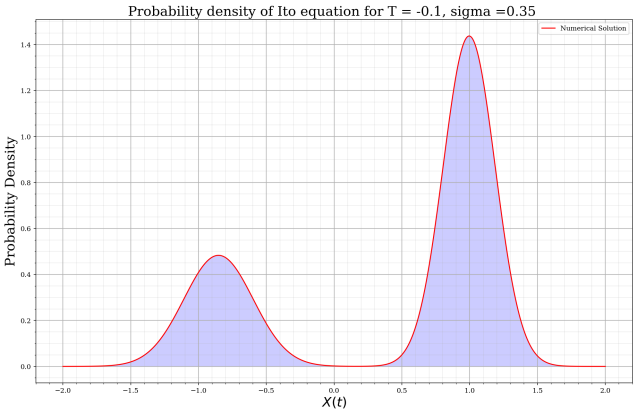

Figure 20: Probability density for intermediate state. $T = -0.1$, $\sigma = 0.35$

All graphs above were used to produce the table in section 3.3.

B Analytical On/Off State solutions

Solutions to on/off states are difficult to find. In this section, solutions of a particular form can be found, but information on the overall structure of these solutions is difficult to determine. By keeping $\mathcal{F}$ non-zero and multiplying equation 4.1.9 through by $\exp\left(\frac{-2}{\sigma^2}U_{max}\right)$,

$$-\exp\left(\frac{-2}{\sigma^2}U_{max}\right)\frac{\sigma^2}{2}\exp\left(\frac{2}{\sigma^2}U\right)\mathcal{F}dX_t = \exp\left(\frac{-2}{\sigma^2}U_{max}\right)\frac{\partial}{\partial X_t}\exp\left(\frac{2}{\sigma^2}U\right)\rho\left(X_t;t\right), \quad \text{(B.0.1)}$$

integrating with respect to dX_t around the maxima,

$$\int -\frac{\sigma^2}{2}\exp\left(\frac{2}{\sigma^2}\left[U-U_{max}\right]\right)\mathcal{F}dX_t = \int \exp\left(\frac{2}{\sigma^2}\left[U-U_{max}\right]\right)d\rho\left(X_t;t\right).$$

Taylor expanding U about $U(X;T)|_{X=X_{max}}$,

$$U(X;T) = \sum_{n=0}^{\infty}\frac{1}{n!}\frac{d^nU(X;T)}{dX^n}|_{X=X_{max}}\left(X-X_{max}\right), \quad \text{(B.0.2)}$$

$$= U(X_{max};T) + \left(X-X_{max}\right)\frac{dU(X;T)}{dX} + \left(X-X_{max}\right)^2\frac{1}{2!}\frac{d^2U(X;T)}{dX^2} + \mathcal{O}\left(\left(X-X_{max}\right)^3\right),$$

therefore,

$$U-U_{max} = \left(X-X_{max}\right)\frac{dU(X;T)}{dX} + \left(X-X_{max}\right)^2\frac{1}{2!}\frac{d^2U(X;T)}{dX^2} + \mathcal{O}\left(\left(X-X_{max}\right)^3\right).$$

Inserting the remaining non-zero leading order terms into the equation for ρ,

$$\int -\frac{\sigma^2}{2}\exp\left(\frac{1}{\sigma^2}\left[\left(X-X_{max}\right)^2\frac{d^2U(X;T)}{dX^2}\right]\right)\mathcal{F}dX_t = \int \exp\left(\frac{2}{\sigma^2}\left[U-U_{max}\right]\right)d\rho \quad \text{(B.0.3)}$$

Consider the limits where $X < X_{max}$ and $X > X_{max}$ as upper and lower limits respectively,

$$-\int_{X<X_{max}}^{X>X_{max}}\frac{\sigma^2}{2}\exp\left(\frac{1}{\sigma^2}\left[\left(X-X_{max}\right)^2\frac{d^2U(X;T)}{dX^2}\right]\right)\mathcal{F}dX_t = \left[\exp\left(\frac{2}{\sigma^2}\left[U-U_{max}\right]\right)\rho\right]_{X<X_{max}}^{X>X_{max}}. \quad \text{(B.0.4)}$$

Rearranging the left-hand side of the equation into the form,

$$-\frac{\mathcal{F}}{2\sigma^2}\int_{X<X_{max}}^{X>X_{max}}\exp\left(\left[\frac{\left(X-X_{max}\right)}{\sigma}\sqrt{\frac{d^2U(X;T)}{dX^2}}\right]^2\right)dX_t \quad \text{(B.0.5)}$$

means that the Gaussian error function can be used to solve the integral.

$$\int_0^{\gamma}\exp\left(-\gamma^2\right)d\gamma = \frac{\pi}{2}erf\left(\gamma\right). \quad \text{(B.0.6)}$$

In the case of the probability density, the integral is now,

$$\left[\exp\left(\frac{2}{\sigma^2}\left[U-U_{max}\right]\right)\rho\right]_{X<X_{max}}^{X>X_{max}} = \left[-\frac{\mathcal{F}}{\pi\sigma^2}erf\left(\frac{\left(X-X_{max}\right)}{\sigma}\sqrt{\frac{d^2U(X;T)}{dX^2}}\right)\right]_{X<X_{max}}^{X>X_{max}}. \quad \text{(B.0.7)}$$

Plotting the right-hand distributions and left-hand distributions matches figure **??**.